Proceedings of the 17th World Congress
The International Federation of Automatic Control
Seoul, Korea, July 6-11, 2008

Modelling and Control of Consumable Double-Electrode Gas Metal Arc Welding Process

Kehai Li and YuMing Zhang

Center for Manufacturing and
Department of Electrical and Computer Engineering
University of Kentucky, Lexington, KY 40506 USA
(email: Kehai.Li@uky.edu, Yuming.Zhang@uky.edu)

Abstract: Consumable double-electrode gas metal arc welding (DE-GMAW) is an innovative process, which offers unique advantages to increase productivity and reduce heat distortion. However, it must be appropriately feedback controlled for any practical use. To this end, the authors identified two critical variables as outputs for the control system to be developed. The control variables were then selected to ease the modeling and control design through establishing two decoupled SISO subsystems. Each SISO subsystem was modeled as an interval model, whose parameters were unknown but bounded by known intervals. The intervals were obtained through a set of designed step response experiments. A prediction based interval model control algorithm was then implemented to control the resultant interval models. Closed-loop control experiments verified the effectiveness of the developed control system for this novel welding process.

1. INTRODUCTION

To maintain the competitiveness and technological leadership, manufacturing industry continuously looks for novel processes to increase welding productivity and reduce welding distortion. Gas metal arc welding (GMAW) is one of the major welding processes used to join metals. Its variants such as Tandem GMAW (Ueyama et al., 2005, Tsushima and Kitamura, 1996), Variable-Polarity GMAW (Talkington, 1998, Cary and Chaisson, 1986, Tong et al., 2001, Harwig et al., 2006), and T.I.M.E. (Transferred Ionized Molten Energy) GMAW (Church, 2001, Lahnsteiner, 1992) have been studied and implemented to increase the productivity and reduce heat distortion. However, all of them share the same operation principle with conventional GMAW process: the current which melts the wire and determines the productivity is the same as the current which heats the base metal and generates distortion. As a result, the maximum current permitted for a specific application is restricted. To resolve this fundamental issue and find a way to substantially increase the productivity and reduce the heat input thus the distortion, a novel process referred to as consumable double-electrode GMAW (DE-GMAW) has been developed at the University of Kentucky.

As illustrated in Fig. 1, the consumable DE-GMAW shown in (a) was formed by adding another GMAW torch (which supplies a consumable bypass electrode) and a constant current (CC) welder to a conventional GMAW system as illustrated in (b). The CC welder provides the bypass current I_2 while the constant voltage (CV) welder provides the base metal current I_1. Two consumable wires are fed in by two wire feeders. Two parallel welding arcs are thus present: the main arc established between the main wire and the workpiece, and the bypass arc established between the main wire and the bypass wire. The total current I which melts the main wire thus consists of two parts: the base metal current I_1 which heats the base metal and bypass current I_2 which melts the bypass wire. (Here the base metal current is denoted as I_1 and the bypass current is denoted as I_2. Similarly, V_1, V_2, WFS_1, and WFS_2 denote arc voltage and wire feed speed in the main and bypass system.) This fundamental principle of DE-GMAW can be expressed in an equation as

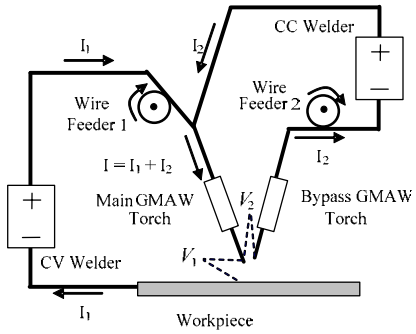

(a) Consumable DE-GMAW

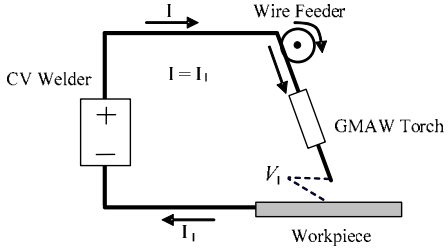

(b) Conventional GMAW

Fig. 1 Consumable DE-GMAW Principle.

$$I = I_1 + I_2 \quad (1)$$

Because the base metal is heated by I_1 and the main wire is melted by $I = I_1 + I_2$, the consumable DE-GMAW provides a unique way to allow a large melting current I be used to burn the main wire at a fast speed for high productivity without supplying excessive heat into the base metal. Further, the base metal current can be controlled at a whatever low level. The base metal heat input is thus controllable to reduce the heat distortion. Hence, the consumable DE-GMAW possesses unique capabilities to increase productivity and reduce distortion at the same time. However, as will be analyzed, without control, the bypass arc may not be maintained to facilitate a successful consumable DE-GMAW process and to achieve the desired base metal heat input. Hence, this paper addresses the modeling and control of this innovative and unique process in order to deploy it as a valid manufacturing process.

2. CONTROL SYSTEM STRUCTURE

The objective of this paper is thus to develop a system to maintain the presence of the bypass arc as well as to control the base metal current at the desired level. This implies that the base metal current is one of the critical variables to be controlled and is thus selected as an output. In addition, an additional variable must be identified to describe the state of the bypass arc. By monitoring and controlling this variable, the bypass arc and the consumable GMAW process will be successfully maintained.

In welding, the arc voltage is proportional to the arc length, i.e., the distance between its anode and cathode (Connor et al., 1987). The voltage V_2 of the bypass arc is thus a measurement of its length. Further, an arc is difficult to establish and maintain if the arc length is too large. The bypass arc can thus be maintained by controlling the bypass arc voltage V_2 at a desired value, which corresponds to an optimal arc length. As a result, the bypass arc voltage V_2 is selected as another output to be feedback controlled. Further, it is found that the optimal voltage corresponding to an optimal length for maintaining the presence of the bypass arc is 1-3volts greater than the main arc voltage V_1 (Li and Zhang, 2007). Hence, the rule for determining the set point for this additional output is also established.

In the consumable DE-GMAW system shown in Fig. 1(a), there are three major variables to control: the main arc voltage V_1, the bypass arc voltage V_2, and the base metal current I_1. However, V_1 is automatically controlled by a controller embedded in the CV welder, which adjusts the current to balance the feeding and melting of the main wire. Hence, in the control system to be developed, the outputs to be controlled are I_1 and V_2. The variables which may be used to effectively change I_1 and V_2 include (1) main wire feed speed WFS_1; (2) bypass wire feed speed WFS_2; (3) main arc voltage V_1; (4) bypass current I_2.

Please note that an ideal CV welder automatically changes the current to maintain the arc voltage at the desired level and an ideal CC welder automatically changes the voltage to maintain the current at the desired level. This implies that I_2 can be freely adjusted as a control variable but I_1 is the result of the action to maintain V_1 at the desired level. However, when WFS_1 is freely changed, the CV welder will automatically change I_1 to balance the feeding and melting of the main wire. Also, when I_2 is freely adjusted, the balance between the feeding and melting of the bypass wire will be changed so that the bypass arc voltage V_2 can be effectively changed.

Careful analysis shows that I_2 and WFS_1 are not only two variables which can be freely adjusted to effectively alter the outputs I_1 and V_2 but also a combination of control variables which can ease the design and development of the control system. In particular, when I_2 is given, WFS_1 only affects I_1. A subsystem SISO system can thus be designed to control I_1 by adjusting WFS_1. Another SISO system will adjust I_2 to control V_2. The resultant control system structure can thus be given in Fig. 2 where pre-filters are used to neutralize the process noises and will be discussed later. It has to be pointed out that a change in I_2 does change I_1. This implies that subsystem 1 (see Fig. 2) does affect subsystem 2. However, the change in I_2 for adjusting V_2 is relatively small and the resultant small change in I_1 does not cause a significant problem for the base metal heat. Further, there is no effect from subsystem 2 to subsystem 1 which requires faster and more accurate control to maintain the bypass arc. Hence, the proposed system structure shown in Fig. 2 establishes the foundation for an effective control of the consumable DE-GMAW process.

3. INTERVAL MODEL CONTROL ALGORITHM

In manufacturing applications, process models are typically affected by manufacturing conditions. Experiments can be conducted to identify models at different manufacturing conditions. If all the models have the same structure but different values for system parameters, an interval can be found for each parameter by using its minimum and maximum values. In this way, the process can be described using an interval model. For interval models, it is not necessary to know the exact values of the parameters, but the range or interval for each parameter must be found for given ranges of manufacturing conditions (Lu et al., 2004). As will be seen in the following discussion, the interval model

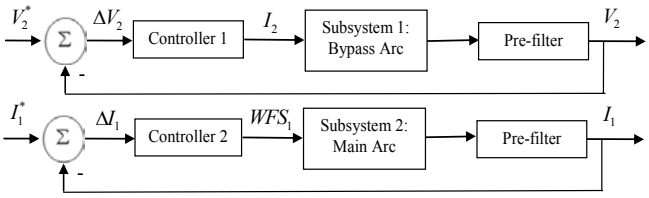

Fig. 2 Proposed Controlled System Structure

control algorithm is a standard program. It does not require any design work but uses the intervals to compute the control variable. Hence, it is suitable for welding engineers without systematical training in control. In particular, for important applications such as the consumable DE-GMAW process, the intervals can be artificially enlarged to increase the stability margin of the closed-loop system.

The original interval model control algorithm (Zhang and Kovacevic, 1997) is based on linear systems described using an impulse response model:

$$y_k = \sum_{j=1}^{N} h(j) u_{k-j} \tag{2}$$

where k is the time instant, y_k is the output at time k, u_{k-j} is the input at time $(k-j)$ $(j>0)$, while N is the system order and $h(j)'s$ are the real parameters of the impulse response function. $h(j)'s$ $(1 \le j \le N)$ are unknown but bounded by intervals:

$$h_{\min}(j) \le h(j) \le h_{\max}(j) \quad (j = 1, \ldots, N) \tag{3}$$

where $h_{\min}(j)$ and $h_{\max}(j)$ are the minimum and maximum value of $h(j)'s$. These boundary values are known. The objective of the interval model control algorithm is to predict the control action u_k such that the closed-loop system achieves the given set-point. Assume the control actions are kept unchanged after instant k, i.e., $\Delta u_{k+j} = 0$ $(\forall j > 0)$. The N-step-ahead predicting yields

$$y_{k+N}(\Delta u_k) = y_k + \sum_{j=2}^{N} h(j)(u_{k-1} - u_{k-j}) + s(N)\Delta u_k \tag{4}$$

where $\Delta u_k = u_k - u_{k-1}$, and $s(i)$ is the unit step response calculated as $s(i) = \sum_{j=1}^{i} h(j)$. The upper and lower limits $s_{\max}(N) = \sum_{j=1}^{N} h_{\max}(j)$ and $s_{\min}(N) = \sum_{j=1}^{N} h_{\min}(j)$ satisfy

$$s_{\max}(N) s_{\min}(N) > 0 \tag{5}$$

It is apparent that

$$y_{k+N}(\Delta u_k) = y_{k+N}(\Delta u_{k-1}) + s(N)\Delta u_k \tag{6}$$

where $y_{k+N}(\Delta u_{k-1}) \triangleq y_{k+N}(\Delta u_k)\big|_{\Delta u_k = 0}$, which is the N-step-ahead prediction of the output made at instant k assuming the control actions are not changed at and after instant k, i.e., $\Delta u_{k+j} = 0$ $(\forall j \ge 0)$. The control action Δu_k is thus determined such that

$$\max y_{k+N}(\Delta u_k) = \max y_{k+N}(\Delta u_{k-1}) + \max(s(N)\Delta u_k) = y^* \tag{7}$$

Because the calculation of $\max y_{k+N}(\Delta u_k)$ requires the input history u and intervals $[h_{\min}(j), h_{\max}(j)]$, the interval model control algorithm does more than an integral control. In addition, it has been proved (Zhang and Kovacevic, 1997) that for the system in (2), the control algorithm described in (7) will yield:

$$\lim_{k \to +\infty} y_k = y^* \tag{8}$$

if the condition $h_{\min}(j) \le h(j) \le h_{\max}(j)$ is satisfied. It is evident that the control algorithm in (7) can be further written as

$$\begin{aligned} \max(s(N)\Delta u_k) &= y^* - \max y_{k+N}(\Delta u_{k-1}) \\ &= y^* - (y_k + \sum_{j=2}^{N} (\max(a,b))) \end{aligned} \tag{9}$$

where $a = h_{\max}(j)(u_{k-1} - u_{k-j})$, $b = h_{\min}(j)(u_{k-1} - u_{k-j})$. Denoting $d_n = \max(s(N)\Delta u_k)$, the control action can be calculated as

$$\Delta u_k = abs(d_n) \min\left(\frac{sign(d_n)}{s_{\max}(N)}, \frac{sign(d_n)}{s_{\min}(N)}\right) \tag{10}$$

where $sign(\bullet)$ is a function to return the sign of its parameter. Then, the control variable can be calculated as $u_k = u_{k-1} + \Delta u_k$.

In a real control system, the control action Δu_k in each step should be limited to a reasonable range, for instance, [-10, 10] for the bypass current, to avoid an abrupt change in u_k. An abrupt change might cause the system unstable. However, this range must be large enough so that the system can respond quickly. Once the new output u_k is calculated, the input history u must be updated. An updated u will be used in the next control cycle. For consumable DE-GMAW, two parallel interval model controllers are needed to control the two parallel subsystems. Each controller has the same structure but takes different parameters and different intervals. Fig. 3 illustrates one of the two controllers based on the interval model control algorithm.

4. SYSTEM MODELLING

Step response experiments were conducted to obtain a model for consumable DE-GMAW. Because systems with different manufacturing conditions may have different models, thus different manufacturing conditions in a large range were used to make sure that the identified models can describe the system dynamics in the whole range of interest.

4.1 Modelling of Bypass Arc Control Subsystem

Fig. 4 illustrates one of the step response experiments for subsystem 1. In these experiments, the main wire feed speed was 14.0m/min (550IPM), and the main arc voltage was set to 36volts. The bypass wire feed speed was 16.5m/min (650IPM). It can be seen that step changes in the bypass current resulted in immediate changes in the bypass arc voltage as well as in the base metal current. However, the total melting current did not change with the bypass current.

Fig. 5 shows the segment when the bypass current was

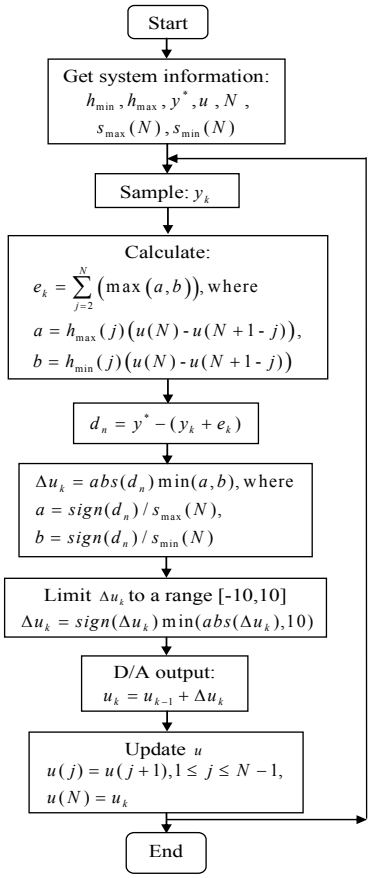

Fig. 3 Flowchart of the interval model control algorithm.

increased from 170amps to 240amps. A careful examination of the step response indicates that (1) the process can be modeled as a first order system; (2) the bypass arc voltage is increased 3.11volts approximately; (The bypass arc voltage was multiplied by a factor 3 such that it can be plotted together with other signals.) (3) the time constant is 0.0228 second approximately. Hence, the resultant model can be expressed in a transfer function $G_1(s) = 0.0444/(0.0228s+1)$ with a static gain equal to 0.0444 V/A. Comparing the simulated V_2 to the actual V_2 in Fig. 5 suggests that the first order system has accurately modeled the process.

More step response experiments were conducted to identify models for subsystem 1. These experiments used different bypass wire feed speeds: high speed at 16.5m/min (650IPM), moderate speed at 10.2m/min (400IPM), and low speed at 5.1m/min (200IPM). Totally, six transfer functions were obtained for subsystem 1: $G_1(s) = 0.0444/(0.0228s+1)$, $G_1(s) = 0.0395/(0.0228s+1)$, $G_1(s) = 0.0449/(0.0270s+1)$, $G_1(s) = 0.0431/(0.0295s+1)$, $G_1(s) = 0.04/(0.0258s+1)$ and $G_1(s) = 0.0414/(0.0277s+1)$. These transfer functions can be easily converted to impulse responses $h_1(t)'s$ by taking the inverse Laplace transform (Rodger E. Ziemer, 1998). Then the discrete impulse response sequence required by the interval model control algorithm can be integrated from the time domain impulse response, i.e., $h_1(j) = \int_{j*ts}^{(j+1)*ts} h_1(t)dt$,

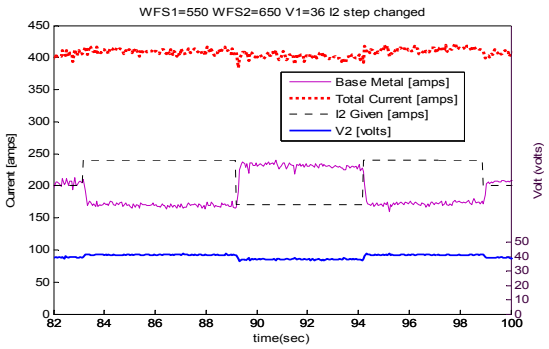

Fig. 4 Step response experiment, $WFS_2 = 650$IPM.

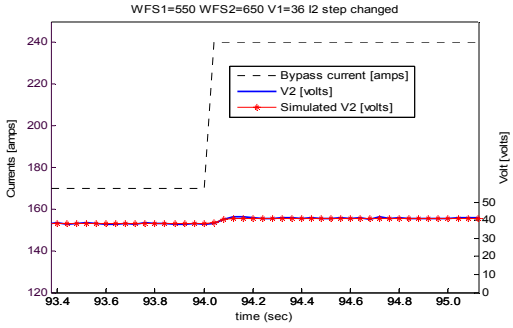

Fig. 5 Step response and simulation.

where ts is the control period. The minimum and maximum values of $h_1(j)'s$ were found to form two curves $h_{1\min}(j) \sim j$ and $h_{1\max}(j) \sim j$. These two curves can be used to give the intervals for the impulse responses. To improve the stability margin of the control system, the resultant intervals are artificially enlarged from $[h_{1\min}(j), h_{1\max}(j)]$ to $[0.8h_{1\min}(j), 1.2h_{1\max}(j)]$. The resultant impulse responses are shown in Fig. 6 with a control period of $ts = 0.01$ second.

4.2 Modelling of Base Metal Current Control Subsystem

Step responses were conducted with different manufacturing conditions to study the dynamics for subsystem 2. During these step response experiments, the bypass arc voltage had to be controlled at 39volts or stable by a single SISO interval model control algorithm. The manufacturing conditions again

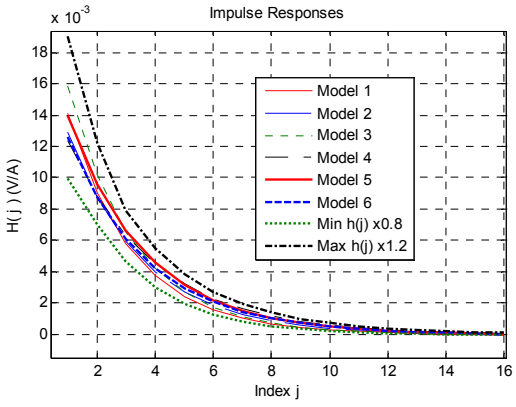

Fig. 6 Impulse responses for subsystem 1.

were selected to assure that the identified model can describe the system dynamics in the whole range of interest. The bypass wire feed speed was fixed at either 8.9m/min (350IPM) or 12.7m/min (500IPM). The main arc voltage was fixed at 36volts.

Fig. 7 demonstrates a step response experiment with a bypass wire feed speed of 8.9m/min (350IPM). While the bypass arc was stable (controlled at 39volts), the main wire feed speed was changed among 12.7m/min (500IPM), 14m/min (550IPM) and 15.2m/min (600IPM) to produce step responses. As expected, the step changes in WFS_1 caused almost identical changes in the base metal current and the total melting current.

Fig. 8 details the step response when WFS_1 was decreased from 15.2m/min (600IPM) to 12.7m/min (500IPM). The base metal current was decreased from 200amps to approximately 175amps. Subsystem 2 thus could be described as a first order system with a static gain of 0.2521 A/IPM and a time constant of 0.0498second. A careful observation showed that a 0.03second delay was introduced due to the mechanical wire feeding system. Thus, this subsystem can be described as $G_2(s) = 0.2521/(0.0498s+1)\exp(-0.03s)$. The simulation of this transfer function demonstrated a good agreement with the experimental data as can be seen in Fig. 8. Similarly, five more models were obtained under different conditions. These six transfer functions were transformed to digital impulse responses to find the intervals.

4.3 Interval Models

In the proposed control system (Fig. 2), the sampled signals will be pre-filtered by a first order filter of $F(s) = 1/(T_f s+1)$,

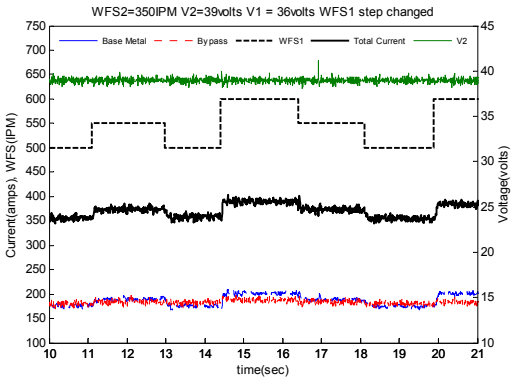

Fig. 7 Step response experiment, WFS_2 = 350IPM.

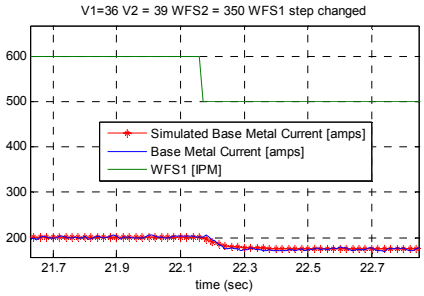

Fig. 8 Step response and simulation.

will be pre-filtered by a first order filter of $F(s) = 1/(T_f s+1)$, where T_f is the time constant and the static gain is 1. This filter can be digitized as $\bar{y}(k) = \alpha\bar{y}(k-1) + (1-\alpha)y(k)$, where $\alpha = \exp(-ts/T_f)$ and ts is the control period (0.01second). Experiments show that the filtering results are satisfactory when T_f = 0.1second (thus $\alpha = 0.9048$). Because of the pre-filters, the two subsystems must be modified as $H_i(s) = G_i(s)F(s), i = 1,2$, resulting in two second order systems. The intervals must be recalculated based on the new transfer functions.

5. EXPERIMENTAL RESULTS AND ANALYSIS

5.1 Experimental Setup

The consumable DE-GMAW system has been described earlier. Two current sensors were added to measure the base metal current and bypass current and two voltage sensors were utilized to measure the bypass arc voltage and main arc voltage. During experiments, the welding torches moved together at a travel speed (TS) of 0.64m/min (25IPM) on 12.7mm (0.5inch) thick low carbon steel workpiece. Pure argon at a flow of 18.9liter/min (40CFH) was used as the shielding gas only from the main torch. Both the bypass arc voltage signal and the base metal current signal were pre-filtered. The two enlarged intervals were used in the close-loop control experiments.

5.2 System Dynamics

Fig. 9 demonstrates the system dynamics when the bypass arc voltage was controlled at 39volts. The bypass wire feed speed was fixed at 10.2m/min (400IPM). This experiment showed how the system responded when the base metal current changed between 180amps and 130amps. As can be seen, the main wire feed speed was reduced when the required base metal current was decreased (approximately at 172second and 183.5second). Potentially, the decrease in the main wire feed speed would increase the main arc voltage. To maintain a constant voltage, the CV power supply automatically decreased the melting current. Because the bypass current was approximately fixed, the required decrease in the base metal current was realized when the total melting current was

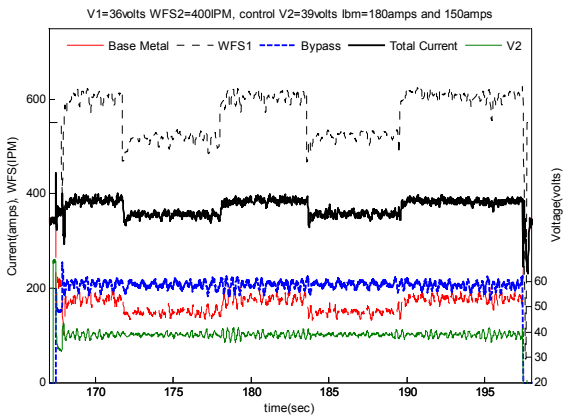

Fig. 9 System dynamics.

decreased. Similarly, when the required base metal current was increased (approximately at 178second and 189.5second), the total melting current was increased by increasing the main wire feed speed by the control algorithm.

5.3 Response to Welding Condition Change

In GMAW, the torch to workpiece distance is a major welding condition subjected to change. A change in this distance would affect the arc voltage, and the melting current will also change when a CV power supply is used. Thus, consumable DE-GMAW must be robust and adjusts the main wire feed speed to maintain the base metal current at the desired level. Fig. 10 shows an experiment designed to test the robustness of the control system with respect to the variations in the torch to workpiece distance. Two pieces (stripes B and D in the figure) of 2.5mm thick mild carbon steel were placed on the top of the 12.7mm (0.5inch) thick workpiece. The welding torches moved from left to right, and the torch to workpiece distance was changed when the torches passed over the two stripes. The control algorithm was able to detect and respond to the change. The welding currents and voltages plotted in Fig. 11 illustrate that the control algorithm successfully controlled both the base metal current and the bypass arc voltage at their desired values.

6. CONCLUSIONS

Consumable double-electrode gas metal arc welding process offers unique advantages but requires appropriate control to operate. The bypass arc voltage and base metal current are identified as the outputs of the control system to be developed. Careful analysis reveals that use of the main wire feed speed and bypass current as control variables can reduce the control problem into the control of two SISO subsystems. To account for different manufacturing conditions, two interval models are obtained, based on experimental data from step responses experiments under different manufacturing conditions, for the subsystems. Experiments verified the effectiveness of the developed interval model control system in achieving a desired consumable DE-GMAW process. The effectiveness of the identified inputs, control variables, and SISO and interval model based control system design in solving a practical problem of the control of a relatively complex manufacturing process is thus also verified.

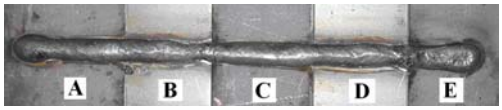

Fig. 10 Experiment with different workpiece thickness.

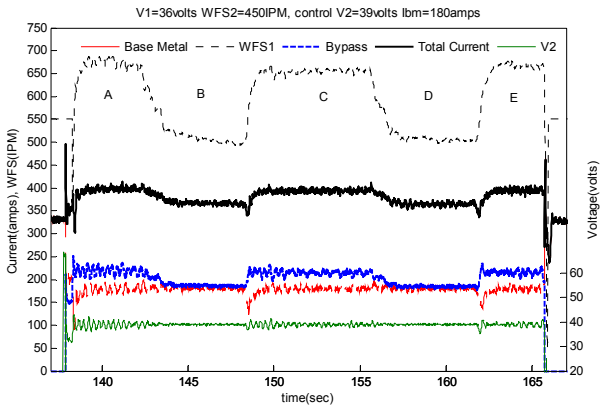

Fig. 11 Response to workpiece thickness changes.

ACKNOWLEDGMENT

This research was funded by the National Science Foundation (NSF) under grant No. DMI-0355324 entitled "Double-electrode gas metal arc welding."

REFERENCES

CARY, H. & CHAISSON, W. (1986) Variable Polarity Plasma Arc Welding. Metairie, LA, USA, Aluminum Assoc, Washington, DC, USA.

CHURCH, J. (2001) T.I.M.E. process produces fracture-proof welds. *Welding Design and Fabrication,* 74**,** 32-35.

CONNOR, L. P., O'BRIEN, R. L. & OATES, W. R. (1987) *Welding handbook,* Miami, FL, American Welding Society.

HARWIG, D. D., DIERKSHEIDE, J. E., YAPP, D. & BLACKMAN, S. (2006) Arc behavior and melting rate in the VP-GMAW process. *Welding Journal,* 85**,** 52S-62S.

LAHNSTEINER, R. (1992) The T.I.M.E. process - an innovative MAG welding process. *Welding Review International,* 11**,** 17-20.

LI, K. H. & ZHANG, Y. M. (2007) Consumable Double-Electrode GMAW, Part I: The Process. *Accepted for publication in Welding Journal.*

LU, W., ZHANG, Y. M. & LIN, W. Y. (2004) Nonlinear interval model control of quasi-keyhole arc welding process. *Automatica,* 40**,** 805-813.

RODGER E. ZIEMER, W. H. T., D. RONALD FANNIN (1998) *Signals & Systems: Continuous and Discrete*, Prentice Hall.

TALKINGTON, J. E. (1998) Variable Polarity Gas Metal Arc Welding. *Welding Engineering.* Columbus, Ohio, The Ohio State University.

TONG, H., UEYAMA, T., HARADA, S. & USHIO, M. (2001) Quality and productivity improvement in aluminum alloy thin sheet welding using alternating current pulsed metal inert gas welding system. *Science and Technology of Welding and Joining,* 6**,** 203-208.

TSUSHIMA, S. & KITAMURA, M. (1996) Tandem electrode AC-MIG welding - development of AC-MIG welding process (report 4). *Welding Research Abroad,* 42**,** 26-32.

UEYAMA, T., OHNAWA, T., TANAKA, M. & NAKATA, K. (2005) Effects of torch configuration and welding current on weld bead formation in high speed tandem pulsed gas metal arc welding of steel sheets. *Science and Technology of Welding and Joining,* 10**,** 750-759.

ZHANG, Y. M. & KOVACEVIC, R. (1997) Robust control of interval plants: A time domain method. *IEEE Proceedings-Control Theory and Applications,* 144**,** 347-353.